JEEE-U Journal of Electrical and Electronic Engineering-UMSIDA
ISSN 2460-9250 (print), ISSN 2540-8658 (online)
Vol. 10, No. 2, October 2026
10.21070/jeeeu.v10i2.1758

Solar-Powered IoT-Based Nutrient Supply Automation for Supporting the Performance of Hydroponic Farming Systems

Otomatisasi Pasokan Nutrisi Berbasis IoT dan Tenaga Surya untuk Mendukung Kinerja Sistem Pertanian Hidroponik

Lailia Rahmawati[1*], Winarti[2], Mohamad Mohsin[3], Agus Fahmi[4], Machrus Ali[5], Dafit Soni Setiawan[6], Soraya Eka Hapsari[7]

[1,2,7] Department of Informatics Engineering, Universitas Darul Ulum, Jombang, Indonesia
[3] Department of Electrical Engineering, Universitas Muhammadiyah Ponorogo, Ponorogo, Indonesia
[4] Department of Agrotechnology, Universitas Darul Ulum, Jombang, Indonesia
[5,7] Department of Electrical Engineering, Universitas Darul Ulum, Jombang, Indonesia
liaundarjombang@gmail.com

ABSTRACT

Reliable nutrient supply is the primary determinant of small-scale hydroponic system performance, yet many Internet of Things (IoT) systems still depend on cloud-based decision making and grid electricity, so they stop working when the network or the power supply is unavailable. This study designed and functionally evaluated a solar-powered IoT nutrient supply automation system for hydroponics. The system integrates an ESP32, a DS3231 real-time clock (RTC), a DHT11 sensor, a Total Dissolved Solids (TDS) sensor, two nutrient dosing pumps, a 40 W submersible pump, a relay module, an LCD, and three-channel reporting through Blynk, Telegram, and Google Spreadsheet every 10 s. The energy layer is a stand-alone photovoltaic plant consisting of a 450 Wp module, a 24 V MPPT solar charge controller, an 8S 25.6 V 100 Ah LiFePO4 battery (2,560 Wh), a 3,000 W inverter, and a 24 V to 5 V DC-DC converter. The novelty is the combination of decision autonomy through 400 ppm threshold dosing, time autonomy through RTC-backed local scheduling, and energy autonomy within one system. Validation covers five dimensions: environmental reading consistency, timekeeping, actuation reliability, monitoring availability, and energy balance adequacy. Testing recorded 29.1-31.2 degrees Celsius, 62-68% RH, 0 s RTC deviation over five days, and 100% schedule execution and actuation reliability. Field monitoring recorded a nutrient decline from 397 to 386 ppm with EC of 0.6000-0.6200 mS/cm. The energy balance shows 1,350 Wh/day of generation against 42 Wh/day (on-demand inverter) or 398 Wh/day (continuous inverter), giving adequacy ratios of 32x and 3.4x. Inverter standby loss, not the pumps, governs the energy balance.

Keywords: *nutrient supply automation; hydroponics; Internet of Things; solar energy; ESP32*

I. INTRODUCTION

Hydroponics is a soilless production approach in which plants obtain water and mineral nutrients from a prepared nutrient solution. Because the roots have no soil nutrient reserve, hydroponic performance is strongly determined by the regularity of nutrient supply: the solution must be circulated at the right time and its concentration must be maintained within a suitable range. In household, classroom, and community-scale units, the most pressing operational problem is not advanced nutrient optimization but the ability to supply and circulate the nutrient solution repeatedly, consistently, and without depending on operator presence. Manual watering or simple timer operation can cause missed supply events, uncorrected concentration decline, and limited information on whether the pump actually worked. Dependence on grid electricity adds another point of failure, because a blackout halts the whole nutrient supply chain. The gap addressed in this study is therefore the need for a low-cost nutrient supply automation baseline that works locally, maintains solution concentration, is powered by solar energy, and still provides simple remote supervision.

IoT technology has accelerated smart agriculture through connected sensors, controllers, actuators, and cloud or mobile dashboards. Greenhouse and irrigation studies have reported IoT benefits for resource management, environmental visibility, and decision support [1], [2]. In hydroponics, recent work increasingly covers pH, electrical conductivity (EC), total dissolved solids (TDS), water level, solution temperature, illumination, flow condition, camera-based monitoring, and artificial-intelligence recommendation [3], [4], [5]. In parallel, solar energy use in irrigation and smart farming has grown because cultivation installations are often located in yards, rooftops, or plots far from electrical connection points, and because small DC controller and pump loads match micro-scale photovoltaic generation well [6], [7]. Such systems are important for precision agriculture, but their calibration, data storage, maintenance, and connectivity requirements may not yet be needed by novice users who first require a reliable, energy-independent nutrient supply layer.

This study focuses on minimum viable automation of hydroponic nutrient supply. Unlike cloud-centric systems whose operation depends on network availability, and unlike prototypes that depend entirely on grid electricity, the proposed system decouples the critical nutrient supply function from two dependencies at once: network dependency and power supply dependency. A battery-backed RTC provides the local time reference, a TDS sensor provides the concentration control variable, the ESP32 executes deterministic rule-based control, the photovoltaic subsystem supplies operating energy, and Blynk visualizes status data when Wi-Fi is available. This local-first and energy-independent design is intended to keep routine nutrient supply running even when the monitoring layer or the power supply is unavailable.

The research questions are: (1) Can an ESP32-DS3231-TDS architecture execute nutrient supply according to a fixed daily schedule while maintaining solution concentration at a defined threshold? (2) Can the prototype present temperature, humidity, nutrient concentration, and pump status consistently both locally and remotely? (3) Can the designed solar power subsystem meet the daily energy demand of that automation system? (4) Which prototype-level indicators can evaluate system performance without overstating agronomic effectiveness?

The contributions are fourfold: a low-cost replicable architecture combining an ESP32, DS3231 RTC, DHT11, TDS sensor, relays, nutrient and water pumps, an LCD, a Blynk dashboard, and a stand-alone photovoltaic supply; the integration of RTC-assisted scheduling and solar powering as the main novelty, so that time and energy for nutrient supply are provided locally rather than through cloud, smartphone, or grid availability; transparent prototype-level metrics covering time error, schedule execution success, actuation reliability, environmental descriptive statistics, nutrient concentration dynamics, and the daily energy balance; and a clear boundary between engineering feasibility and agronomic validation, including the additional measurements required for future claims.

The reviewed literature shows four complementary streams. The first concerns greenhouse and irrigation management at a broad system level [1], [2], whose scope is wider than a compact hydroponic device for household or educational use. The second addresses IoT hydroponics directly through AI-IoT crop recommendation and nutrient parameter monitoring [3], modular IoT hydroponic systems [8], ESP32-based pH, TDS, water-level, and Blynk monitoring [9], and advanced ESP32 NFT architectures with MQTT, InfluxDB, Node-RED, Grafana, and Flutter applications [5]; these demand higher calibration, maintenance, and data-processing effort than an entry-level scheduled irrigation baseline. The third concerns nutrient quality regulation: Sulaiman et al. [10] screened 3,222 studies and analysed 89 on automated dosing, reporting pH (70 studies), EC (36), TDS (27), solution volume (42), and solution temperature (28) as critical variables, confirming that complete dosing systems require calibrated sensors, repeated validation, and reliable dose volume measurement. The fourth emphasises the prototype-to-field gap: low-cost systems such as SMART GROW [11], IoT-enhanced deep water culture [4], and ESP32-Firebase data acquisition [12] prove affordable automation is achievable, while a synthesis of 74 IoT hydroponic studies reports that many systems remain fragmented, ad hoc, and insufficiently standardised for robust real deployment [13].

Accordingly, the novelty claimed here is not a new sensor, a new AI algorithm, or a complete nutrient dosing controller. The contribution is a deployment-oriented integration of concentration-threshold nutrient supply

JEEE-U Journal of Electrical and Electronic Engineering-UMSIDA
ISSN 2460-9250 (print), ISSN 2540-8658 (online)
Vol. 10, No. 2, October 2026
10.21070/jeeeu.v10i2.1758

automation, RTC-backed local scheduling, simple environmental monitoring, mobile supervision, and solar powering in one low-cost prototype. Many smart-farming publications emphasise broad greenhouse automation or soil-based irrigation rather than scheduled, concentration-controlled nutrient supply in small-scale hydroponics; fewer explicitly examine how a local RTC preserves the supply schedule when the IoT dashboard is used mainly for supervision; and fewer still unify that layer with a solar power supply and its energy balance calculation. Finally, prototype articles often report functionality narratively without transparent reliability metrics. This study answers those gaps through RTC- and TDS-assisted local control, solar powering, comparative positioning against cloud-centric systems, and replicable prototype-level validation metrics.

II. METHODS

2.1 Type of Research and Research Design

The study used an experimental prototype development method consisting of problem identification, literature-based gap formulation, hardware design, solar power subsystem design, software development, system integration, and functional evaluation. The scope was limited to validating whether the system can execute a fixed nutrient supply schedule, maintain solution concentration at the defined threshold, display ambient temperature and humidity, actuate the pumps, transmit monitoring information to a mobile IoT interface, and meet daily energy demand from the photovoltaic generator based on an energy balance calculation. Plant growth, pH control, flow rate, water use efficiency, irradiance and battery state-of-charge measurement, and economic feasibility were outside the scope of this prototype-level study. This scope was chosen deliberately, because the objective is to validate the solar-powered nutrient supply automation layer before extending the system to advanced nutrient quality regulation and agronomic trials.

Figure 1. Research flow for design

2.2 Research Location

Prototype assembly and functional testing were carried out in the electrical and informatics engineering laboratory environment of Universitas Darul Ulum, Jombang, East Java, Indonesia. Continuous field monitoring was conducted at the Smart Garden hydroponic installation, an outdoor unit operated under ambient tropical conditions and powered entirely by the stand-alone photovoltaic plant described in Subsection 2.4.

2.3 System Architecture and Materials

The proposed system consists of six functional layers. The sensing layer uses a DHT11 sensor to monitor air temperature and relative humidity and a TDS sensor to measure nutrient solution concentration. The timing layer uses a DS3231 RTC module as a battery-backed local time reference. The DHT11 datasheet states a measuring range of 20-90% RH and 0-50 degrees Celsius with accuracy of about plus or minus 5% RH and plus or minus 2 degrees Celsius [14], while the DS3231 datasheet specifies battery-backed timekeeping with plus or minus 2 ppm accuracy from 0 to plus 40 degrees Celsius [15]. The processing layer uses an ESP32 microcontroller because of its integrated Wi-Fi connectivity and adequate I/O resources for compact IoT prototypes [16], [17]. The actuation layer comprises a relay module, two nutrient dosing pumps, and a 40 W submersible pump. The monitoring layer uses an LCD for local display and the Blynk IoT platform for smartphone observation [18], [19]. The energy layer, which is the main distinguishing feature, comprises a 450 Wp solar module, an MPPT solar charge controller, an 8S 25.6 V 100 Ah LiFePO4 battery, a 3,000 W inverter, and a 24 V to 5 V DC-DC converter, as described in Subsection 2.4.

The architecture follows both local-first and energy-independent principles. Nutrient supply decisions are executed by the ESP32 using DS3231 time data, TDS readings, and programmed rules, while energy is supplied by the photovoltaic subsystem with a battery buffer. Wi-Fi and Blynk are used to transmit and visualise monitoring data, not as the sole time or control reference. This separation matters because nutrient supply events must continue when network availability is intermittent or when grid supply is disturbed [6], [20], [21].

Figure 2. Local-first, solar-powered IoT architecture with RTC-based scheduling.

2.4 Energy Layer: Solar Power Subsystem

Unlike hydroponic prototypes commonly powered from the grid, this system is designed so that all control and actuation loads are served

JEEE-U Journal of Electrical and Electronic Engineering-UMSIDA
ISSN 2460-9250 (print), ISSN 2540-8658 (online)
Vol. 10, No. 2, October 2026
10.21070/jeeeu.v10i2.1758

by a stand-alone photovoltaic (PV) plant on a 24 V bus. The 450 Wp module acts as the primary generator; because the maximum operating voltage of this module class is around 40 V, charging uses a maximum power point tracking (MPPT) solar charge controller (SCC) with at least 20 A output rather than a PWM type, so that the module-to-bus voltage difference is converted into charging current instead of being lost. Energy storage uses an 8S lithium iron phosphate (LiFePO4) battery with 25.6 V nominal voltage and 100 Ah capacity, equal to 2,560 Wh of stored energy, equipped with a battery management system (BMS) for cell balancing and voltage, current, and temperature protection. LiFePO4 chemistry was chosen because the permissible depth of discharge reaches 80% or more, cycle life is in the thousands of cycles, the discharge curve is relatively flat so the bus voltage is more stable, and charging losses are lower than lead-acid [22]. The 8S configuration requires an SCC supporting a LiFePO4 charging profile, that is an absorption voltage of about 28.8 V (3.6 V per cell) without a prolonged float stage, so the BMS does not repeatedly trip protection. A Taffware 3,000 W inverter, with 15 W standby loss per manufacturer specification, provides 220 V AC output for the submersible pump and other AC loads, while a 24 V to 5 V step-down DC-DC converter powers the ESP32, sensors, and LCD directly from the DC bus so that the control layer stays alive independently of the inverter.

Component sizing was evaluated through an energy balance calculation. The continuously operating control load, that is the ESP32 with Wi-Fi, DHT11, TDS sensor, RTC, and LCD, draws about 1.5 W on average, requiring about 36 Wh per day. The actuation load consists of the 40 W submersible pump operating twice a day for one minute, equal to 1.3 Wh per day, plus two nutrient dosing pumps operating in short cycles of a few seconds with a demand below 1 Wh per day; accounting for an inverter conversion efficiency of about 85%, the total actuation load remains below 3 Wh per day. The dominant component is instead the standby loss of the 3,000 W inverter, specified at 15 W, equal to about 360 Wh per day if the inverter is left on for 24 hours. The system was therefore designed with two operating scenarios: an economical scenario in which the inverter is activated only about 15 minutes per day during pump cycles, giving a daily demand of about 42 Wh/day, and a continuous-inverter scenario with a demand of about 398 Wh/day. On the generation side, the 450 Wp module with an assumed four peak sun hours and a combined derating factor of 0.75 for temperature losses, soiling, SCC efficiency, and charging efficiency can potentially produce about 1,350 Wh/day [7]. The 2,560 Wh LiFePO4 battery at 80% depth of discharge provides about 2,048 Wh of usable energy, equal to about 49 days of autonomy in the economical scenario or about 5.1 days in the continuous-inverter scenario. For comparison, a lead-acid battery of the same nominal capacity provides only about 1,280 Wh of usable energy at 50% depth of discharge, so the LiFePO4 choice increases usable energy by about 60% without adding nominal capacity.

The 3,000 W inverter rating far exceeds the peak load of this hydroponic system, which is only about 40 W when the submersible pump runs alone or below 150 W when all pumps run together. The choice remains defensible because the submersible pump draws a starting surge several times its rated current, surplus capacity provides headroom for future expansion, and in yard installations the same PV plant is often shared with household loads. The consequence is an inverter loading factor of only about 1.3% of installed capacity when serving the submersible pump, so conversion efficiency is low and standby loss dominates. Demand-based operation, that is inverter switching by a scheduled relay from the ESP32, or a 24 V DC submersible pump fed directly from the battery bus, is therefore the most decisive efficiency improvement. Overall, time autonomy comes from the battery-backed RTC, decision autonomy from rule-based control on the ESP32 with TDS input, and energy autonomy from the 450 Wp PV plant with a 2,560 Wh LiFePO4 buffer; all three operate on different layers but converge on keeping nutrient supply running when external services are unavailable.

Table 1. Prototype components, including the solar power subsystem, and their functional roles.

2.5 Hardware Implementation

The ESP32 acts as the main controller. The DHT11 data pin is connected to GPIO 4. The TDS sensor is connected to an ESP32 analogue input channel to read nutrient concentration. The DS3231 RTC communicates with the ESP32 over I2C and provides the local time base. Relay inputs are connected to digital output pins and

Journal of Electrical and Electronic Engineering-UMSIDA
ISSN 2460-9250 (print), ISSN 2540-8658 (online)
Vol. 10, No. 2, October 2026
10.21070/jeeeu.v10i2.1758

switch the nutrient dosing pumps and the 40 W submersible pump. The LCD displays time, environmental readings, nutrient concentration, and pump status. All modules are assembled on a prototyping board and powered from the 24 V PV bus: the 220 V output of the Taffware 3,000 W inverter feeds the pumps through the relay module, while a 5 V rail derived from the 24 V to 5 V DC-DC conversion feeds the controller, sensors, and LCD, so the control layer keeps operating while the inverter is off.

The DHT11 is used only as a low-cost contextual sensor, because this prototype targets household- and education-scale replication. Its datasheet states a 20-90% RH range, a 0-50 degrees Celsius temperature range, and typical accuracy limits of about plus or minus 5% RH and plus or minus 2 degrees Celsius [14]; DHT11 data are therefore interpreted as evidence of display consistency, not as formal accuracy validation. The DS3231 was selected because it provides a battery input for continuous timekeeping when main power is interrupted and is specified at plus or minus 2 ppm accuracy from 0 to plus 40 degrees Celsius [15]. The TDS sensor was chosen as the nutrient supply control variable because solution concentration most directly represents nutrient availability to plants, consistent with the variables most frequently reported in automated nutrient dosing frameworks [10].

Figure 3. DHT11- and ESP32-based environmental monitoring subsystem, and DS3231 RTC integration for local timekeeping.

2.6 Software and Control Logic

The control software was developed in the Arduino IDE using C/C++. The program performs five main operations: reading temperature and humidity from the DHT11, reading solution concentration from the TDS sensor, retrieving current time from the DS3231, comparing RTC time with the programmed nutrient supply schedule and comparing the TDS value with the concentration threshold, and switching the relays to turn the pumps on or off. Supply events are scheduled at 07:00 and 16:00. Placing both events within daylight hours is also energetically advantageous, because most of the pump load can be served directly by the module output, reducing battery discharge cycles.

Table 2. Rule-based control sequence implemented on the prototype.

2.7 Data Collection Technique

The validation protocol was arranged in five dimensions: environmental reading consistency, RTC timekeeping consistency, nutrient supply pump actuation reliability, IoT monitoring availability, and solar power energy balance adequacy. Simple quantitative indicators derived from prototype observation were used instead of narrative statements alone. The available dataset comprises four daytime DHT11 readings, five daily RTC time checks, two scheduled pump activation events, four observed pump ON/OFF states, and PPM and EC time-series data from field monitoring logged automatically every 10 s. The energy dimension was evaluated through an energy balance calculation based on component specifications and nominal load profiles rather than field irradiance measurement.

Table 3. Prototype evaluation dimensions and metrics.

2.8 Data Analysis

Time error is the absolute difference between RTC time and reference time. Schedule execution success is the number of successful scheduled pump activations divided by the number of programmed activation events. Actuation reliability is the number of correct pump states divided by the number of observed pump state events. For DHT11 readings, descriptive statistics were computed from recorded values. For the energy dimension, daily energy demand was computed as E_load = sum of (P_i multiplied by t_i), where P_i is the nominal power of each load and t_i its daily operating duration; daily PV production potential as E_PV = P_STC multiplied by PSH multiplied by eta, where PSH is peak sun hours and eta the combined derating factor; the energy adequacy ratio as E_PV divided by E_load; and battery autonomy as (C multiplied by V multiplied by DoD) divided by E_load. Because the number of observations is small, the analysis was limited to means, ranges, sample standard deviations, coefficients of variation, percentage-based reliability indicators, and deterministic energy balance computation. Accordingly, the DHT11 analysis is interpreted as a consistency test rather than formal accuracy validation, and the RTC result represents short-term time consistency rather than long-term oscillator drift. Pump testing verifies time-based actuation but not the delivered nutrient volume per cycle, because

ISSN 2460-9250 (print), ISSN 2540-8658 (online)
Vol. 10, No. 2, October 2026
10.21070/jeeeu.v10i2.1758

flow rate was not measured. Stronger statistical validation would require at least 30 repeated observations per key variable, an observation period of several weeks, and additional variables such as flow rate, nutrient volume, pH, EC or TDS, dashboard update latency, packet delivery ratio, and reconnection time.

III. RESULTS AND DISCUSSION

3.1 Prototype Implementation

The prototype was successfully assembled by integrating the ESP32, DHT11, TDS sensor, DS3231, relay module, nutrient and DC water pumps, LCD, Blynk monitoring interface, and the solar power subsystem. Sequential testing verified that the ESP32 could read environmental and concentration data, retrieve time from the RTC, drive the relays according to the programmed schedule and threshold, transmit status data to the IoT interface, and operate on power sourced from the solar module through the SCC and battery.

Figure 4. Integrated hydroponic nutrient supply automation prototype with relays, pumps, solar power supply, and the Blynk IoT monitoring interface.

3.2 Environmental Monitoring Using the DHT11

The DHT11 produced periodic temperature and humidity readings displayed on the LCD, Serial Monitor, and Blynk interface. Temperature ranged from 29.1 to 31.2 degrees Celsius and relative humidity from 62 to 68%. These values reflect environmental variation around the prototype during daytime observation rather than sensor accuracy in a controlled test chamber. The results therefore support display consistency for contextual monitoring but cannot be treated as evidence of calibrated sensing accuracy.

Table 4. DHT11 test results and descriptive statistics.

The coefficients of variation were 3.08% for temperature and 4.11% for relative humidity, and no visible discrepancy was found between the LCD, Serial Monitor, and Blynk displays during testing, indicating that the sensing and display chain functioned consistently. This must not be interpreted as calibrated accuracy, because no reference instrument was used.

Figure 5. DHT11 temperature and humidity trend during the daytime observation window.

3.3 DS3231 Timekeeping and Scheduling

The DS3231 provided the local time reference for irrigation scheduling, which is beneficial because the pump schedule is preserved even when Wi-Fi monitoring is unavailable. The module is technically suitable for that role because it integrates a temperature-compensated crystal oscillator, a battery backup input, and specified plus or minus 2 ppm accuracy from 0 to plus 40 degrees Celsius [15]. Over five observation days, the recorded deviation at the daily reference point (07:00) was 0 s for all observations, giving a mean absolute time error of 0 s within the resolution limit of the observation method. This five-day observation supports the functional suitability of the DS3231 for short-term scheduled irrigation. The result must be interpreted cautiously, because testing used a prototype-level operational reference and did not measure long-term oscillator drift. Stronger validation should compare the RTC with an internet time server or a calibrated reference over several weeks and report drift in seconds per day, since small drift can accumulate and eventually shift irrigation events during long-term unattended operation.

3.4 Automatic Nutrient Supply Actuation

The relays and nutrient pumps were tested to verify whether pump state followed the DS3231-based schedule. The system was programmed to activate the pump at 07:00 and 16:00 for 10 s. Both scheduled ON events occurred, and the pump returned to the OFF state after the programmed duration.

Table 5. Automatic nutrient supply test results.

Schedule execution success reached 100% for the two programmed activation events observed, and actuation reliability also reached 100% for the four observed pump state events, confirming correct interaction among the ESP32, DS3231, relay, and pump. The main limitation is that the actual nutrient volume delivered in each 10 s actuation was not measured. The result therefore confirms time-based pump control but not irrigation dose accuracy. Flow sensors or gravimetric output measurement should be added to quantify millilitres per cycle, pump repeatability, output variability, and total daily nutrient volume. Without such measurement, the prototype should be described as a scheduled circulation system rather than a precision nutrient dosing system.

JEEE-U Journal of Electrical and Electronic Engineering-UMSIDA
ISSN 2460-9250 (print), ISSN 2540-8658 (online)
Vol. 10, No. 2, October 2026
10.21070/jeeeu.v10i2.1758

3.5 IoT Monitoring and Integration

The Blynk-based IoT interface displayed temperature, humidity, and pump status during prototype testing. Wi-Fi connectivity was available throughout the test sessions, and the monitored values appeared on the smartphone interface, confirming that the remote monitoring layer functioned in the test environment. The IoT result is useful for remote visibility, because users can check whether the prototype is operating without physically accessing the hydroponic unit. The evaluation nonetheless remains qualitative. Stronger IoT validation requires network performance measurement using dashboard update latency, packet delivery ratio or transmission success rate, reconnection time after Wi-Fi loss, and cloud dashboard uptime. Communication system evaluation in IoT agriculture commonly considers packet delivery ratio, energy consumption, and packet collision, while latency and connectivity quality are also relevant for real-time monitoring [23].

3.6 Solar Power Subsystem Performance

The PV subsystem was evaluated through the daily energy balance, because irradiance and battery state-of-charge instrumentation was not yet available. Based on the load profile in Subsection 2.4, daily energy demand is about 42 Wh/day when the inverter is operated only during pump cycles and about 398 Wh/day when the inverter runs continuously. The 356 Wh/day difference between the two scenarios comes entirely from the standby loss of the 3,000 W inverter. In the economical scenario the load composition is about 86% continuously operating control and sensing load, about 5% pump actuation load, and the remainder inverter standby loss during brief activation periods. This finding is engineering-significant, because it shows that the determinant of energy demand in small-scale nutrient supply automation is not the submersible pump, which draws only about 1.3 Wh/day owing to its very short operating time, but the standby load of the power conversion device together with the continuously operating control load.

The 450 Wp module can potentially produce about 1,350 Wh/day at four peak sun hours and a derating factor of 0.75, so the energy adequacy ratio reaches about 32 times the daily demand in the economical scenario and about 3.4 times in the continuous-inverter scenario. Both values satisfy the adequacy criterion; even in the rainy season, when peak sun hours may halve, the system remains in surplus, so the risk of a daily energy deficit is low. The 2,560 Wh LiFePO4 battery at 80% depth of discharge provides about 2,048 Wh of usable energy, equal to about 49 days of autonomy in the economical scenario and about 5.1 days in the continuous-inverter scenario. Roughly five days of autonomy in the worst case is an adequate margin for consecutive overcast periods in tropical regions, and this is a direct consequence of choosing LiFePO4 chemistry with 80% permissible depth of discharge; with a lead-acid battery of the same nominal capacity, autonomy in the same scenario would be only about 3.2 days. The comparison shows that inverter operating strategy influences system efficiency far more than adding module or battery capacity. Scheduling nutrient supply at 07:00 and 16:00 also aligns with solar availability, since both events fall within daylight hours.

Three engineering recommendations follow: switching the inverter with an ESP32-controlled relay activated only a few minutes before pump cycles, which reduces daily energy demand by about 89% from 398 Wh/day to 42 Wh/day; continuing to feed the control load through the DC-DC converter from the 24 V bus so monitoring, scheduling, and IoT reporting are unaffected when the inverter is off; and replacing the AC pump with an equivalent 24 V DC submersible pump, which removes the inverter and its conversion losses from the nutrient supply chain altogether. It must be re-emphasised that all figures in this subsection result from an energy balance calculation based on component specifications and typical irradiation assumptions, not from field measurement. Stronger validation requires logging of charging current and voltage, delivered daily energy, measured inverter standby consumption, BMS-reported state of charge, and the number of protection trips over at least one month spanning both dry and rainy seasons [7].

3.7 Smart Garden Field Monitoring

As a continuation of the functional validation above, the prototype was operated in continuous monitoring mode at the Smart Garden installation with server-side timestamped logging. Unlike the point-in-time prototype testing (four DHT11 readings in Table 4), field monitoring produced a high-density time series

JEEE-U Journal of Electrical and Electronic Engineering-UMSIDA
ISSN 2460-9250 (print), ISSN 2540-8658 (online)
Vol. 10, No. 2, October 2026
10.21070/jeeeu.v10i2.1758

enabling assessment of environmental trends, nutrient concentration dynamics, and the integrity of the data transmission chain. At this stage the system also included solution quality sensing through parts per million (PPM) and electrical conductivity (EC), the two parameters identified earlier as development needs.

The Smart Garden installation extends the prototype in three respects, which are also the main strengths of this study. First, data reporting uses three complementary channels: the Blynk dashboard, Telegram notifications, and automatic logging to Google Spreadsheet every 10 s. The Blynk dashboard is passive because it must be opened by the user; Telegram adds event-driven push notifications when the concentration threshold is crossed or a pump runs, shifting management from periodic inspection to management by exception; and 10 s logging yields about 8,640 records per day per parameter, far above the recommended minimum of 30 repeated measurements per key metric [10], while removing transcription error and making the record auditable. Together the three channels form a monitoring-alerting-logging pattern rarely satisfied simultaneously by low-cost hydroponic prototypes, which commonly stop at data display without adequate archiving or alerting [13]. Second, TDS sensing makes nutrient concentration a control variable rather than merely an observed one. Third, water irrigation and nutrient dosing were separated into different actuators and control logics.

Table 6. Smart Garden sensor and actuator configuration and control roles.

In automatic mode two control loops run in parallel on different principles. The first is closed-loop, threshold-based nutrient dosing: when the TDS reading falls below the 400 ppm setpoint, nutrient pumps A and B are activated alternately for 5 s each with a 1 s interval between them. The alternating scheme prevents concentrates A and B from meeting while concentrated, since calcium in concentrate A can react with sulphates and phosphates in concentrate B and form precipitates; the 1 s interval allows both solutions to mix in the reservoir; and repeated short doses implement incremental dosing that reduces overshoot beyond the setpoint [10]. The second is open-loop scheduled water irrigation: the water pump runs at 07:00 and 16:00 for 1 min using a dual time reference, the DS3231 as local clock and NTP through the ESP32 as synchroniser when the network is available. This combination strengthens the local-first argument: NTP provides absolute time accuracy while online, whereas the battery-backed RTC guarantees that the schedule continues when the network is lost. This configuration refines the initial prototype setting of one nutrient pump for 10 s into a separation between a 1 min scheduled water pump and threshold-based nutrient pumps. The DHT11 was deliberately excluded as an actuation trigger, consistent with its plus or minus 2 degrees Celsius and plus or minus 5% RH tolerance [14], which is adequate for trend monitoring but not for actuation decisions; its data are treated as context that helps interpret solution dynamics, such as evaporation rate at high temperature.

The system also provides a manual mode in the Blynk interface, with direct on/off switches for the water pump and nutrient pumps A and B, a one-shot 1 min watering action button that standardises manual watering and prevents a pump from running continuously if the user forgets to switch it off, and an Automatic/Manual selector that acts as a mode arbiter so only one command source is active at a time. Both features reflect fail-safe design in embedded systems.

Field monitoring results are summarised in Table 7. Air temperature fluctuated between 28.6 and 30.0 degrees Celsius and relative humidity between about 60 and 71%, with the negative temperature-humidity correlation expected in the literature visible at several early fluctuation points. PPM and EC were logged mainly between 19:28 and 21:51 local time, showing a gradual concentration decline from about 397 to 386 ppm, while EC moved almost identically to PPM within 0.6000-0.6200 mS/cm, consistent with PPM being an estimate derived from solution conductivity through a conversion factor. A logging gap between 2 and 6 August was also observed, which must be considered when evaluating the reliability of the data transmission chain. The slow night-time decline in PPM and EC indicates nutrient uptake by the plants or possible dilution and dissolution caused by other factors, such as water pump operation.

Table 7. Summary of Smart Garden field monitoring parameters.

Figure 6. Smart Garden monitoring of (a) temperature and humidity and (b) nutrient

JEEE-U Journal of Electrical and Electronic Engineering-UMSIDA
ISSN 2460-9250 (print), ISSN 2540-8658 (online)
Vol. 10, No. 2, October 2026
10.21070/jeeeu.v10i2.1758

concentration (PPM and EC)

3.8 Synchronisation with the Prototype Test Results

The field monitoring results agree with the prototype test findings and extend them in three respects, as summarised in Table 8. Environmentally, the field temperature range of 28.6-30.0 degrees Celsius overlaps the earlier DHT11 range of 29.1-31.2 degrees Celsius, and the field humidity range of about 60-71% encompasses the earlier 62-68%, reinforcing the conclusion that the sensing and display chain works consistently, although neither range has been verified against a calibrated reference instrument. Regarding timing, the 0 s DS3231 error over five days shows that the local time reference was preserved, whereas the 2-6 August logging gap is a problem in the data transmission and server storage layer, not in the local scheduling layer. This is empirical evidence for the local-first argument: when the network-based monitoring chain breaks, irrigation scheduling is still executed by the ESP32 with the DS3231, independently of server availability. Regarding actuation and nutrient quality, the PPM decline from about 397 to 386 over roughly 2.4 hours complements the earlier 100% time-based actuation success without dose measurement: recorded concentration change shows that scheduled circulation does affect solution dynamics, but the pump contribution cannot yet be separated from plant uptake or evaporation. The recommendation on flow rate and gravimetric volume measurement therefore still applies, with the additional proposal that PPM/EC logging be synchronised with pump event timestamps so that the effect of each irrigation cycle can be quantified directly.

Table 8. Synchronisation of prototype testing (Subsections 3.2-3.6) and field monitoring (Subsection 3.7).

Methodologically, the validation dimensions in Table 3 should be extended with two additional dimensions: data time-series integrity (record completeness against the expected number of records, longest gap duration, and recovery time) and solution quality consistency (rate of PPM/EC change per unit time and consistency of the PPM-to-EC conversion ratio). Both can be measured from data already available in the existing logs, so their adoption requires no significant additional hardware except for flow rate measurement.

3.9 Discussion, Practical Implications, and Limitations

The results show that a simple ESP32 architecture assisted by an RTC, a TDS sensor, and a solar power supply can support hydroponic nutrient supply automation with remote monitoring. Compared with broader greenhouse IoT systems, the proposed system has a narrower scope but is easier to replicate and does not require a permanent electrical connection. Compared with AIoT, pH/EC-controlled, or cloud-centric hydroponic systems, including ESP32-MING architectures supporting multi-parameter sensing, flow verification, time-series storage, dashboards, and mobile applications [5], this system does not attempt to optimise crop selection or dose volume precisely. Instead it contributes a practical baseline for reliable, autonomous nutrient supply: local RTC timekeeping, a TDS concentration threshold, and solar energy that remain available even when cloud monitoring and the grid are not. The DS3231-solar combination is the most important architectural feature, because it decouples nutrient supply execution from two external dependencies at once, making the system suitable for yard installations, school laboratories, and community demonstrations where internet quality, electricity reliability, technical support, and maintenance resources are limited [6], [7]. Because the control logic is rule-based, users can adjust timing, duration, and concentration thresholds without changing the hardware architecture.

The DHT11 results also highlight a limitation: temperature and humidity are contextual variables that do not directly regulate nutrient concentration, whereas pH, EC or TDS, solution temperature, and solution volume are far more relevant for hydroponic nutrient management [10]. The system should therefore be presented as a scheduled nutrient irrigation prototype rather than a complete nutrient quality control system, and because the same 10 s pump duration can deliver different volumes depending on pump type, hose resistance, head, and supply voltage, flow measurement is required before use in precision dosing.

The study has several limitations. Sensor testing used only four daytime observations without a calibrated reference instrument. RTC testing covered only five days and did not measure long-term drift. Actuation testing observed pump state but did not measure

JEEE-U Journal of Electrical and Electronic Engineering-UMSIDA
ISSN 2460-9250 (print), ISSN 2540-8658 (online)
Vol. 10, No. 2, October 2026
10.21070/jeeeu.v10i2.1758

delivered water or nutrient volume. IoT testing verified display availability but did not quantify network quality such as latency, packet delivery ratio, reconnection time, or success rate. The energy dimension was evaluated through a specification-based energy balance rather than measurement of irradiance, charging current, battery voltage, or state of charge, so the energy adequacy claim must be read as a design outcome and not as measured performance. Finally, no pH or plant growth experiments were conducted; part of the solution-quality sensing limitation was subsequently addressed through PPM and EC monitoring in Subsection 3.7. Future validation should use at least 30 repeated measurements per key metric and include calibrated sensors, gravimetric flow or volume testing, pH/EC monitoring, solar energy data logging, and quantitative IoT performance measurement [7], [10], [23], plus controlled plant growth trials comparing manual irrigation, timer-only irrigation, and RTC-IoT scheduled irrigation using measurable plant variables. Scale should also be extended from a single prototype to several hydroponic units, including classroom- or community-scale deployment, to evaluate scalability and maintenance requirements.

IV. CONCLUSION

This study designed and functionally evaluated a solar-powered IoT-based hydroponic nutrient supply automation system integrating an ESP32 controller, a DS3231 RTC, DHT11 and TDS sensors, relay-controlled nutrient dosing pumps and a 40 W submersible pump, an LCD, a Blynk monitoring interface, and a stand-alone PV plant comprising a 450 Wp module, a 24 V MPPT SCC, an 8S 25.6 V 100 Ah (2,560 Wh) LiFePO4 battery, a 3,000 W inverter, and a 24 V to 5 V DC-DC converter. The prototype executed programmed supply events at 07:00 and 16:00, displayed temperature and humidity, and transmitted monitoring information to a mobile interface. DHT11 readings ranged from 29.1 to 31.2 degrees Celsius and 62 to 68% RH, the DS3231 recorded 0 s deviation at the reference time over five observation days, and pump actuation reliability reached 100% for the observed ON/OFF states. The energy balance indicates about 1,350 Wh/day of production against 42 Wh/day with on-demand inverter operation (ratio about 32 times; autonomy about 49 days) or 398 Wh/day with a continuously energised inverter (ratio about 3.4 times; autonomy about 5.1 days), noting that these figures are design calculations not yet verified by field measurement.

Follow-up monitoring at the Smart Garden installation reinforced and extended these findings. Field temperature was 28.6-30.0 degrees Celsius and relative humidity about 60-71%, overlapping the prototype test results and showing consistency between observation sessions. Nutrient concentration declined gradually from about 397 to 386 ppm with EC of 0.6000-0.6200 mS/cm moving almost identically with PPM. A data logging gap between 2 and 6 August was found in the server transmission layer rather than in the local scheduling layer, providing empirical evidence for the main argument that separating RTC-assisted local scheduling from network-based monitoring is the appropriate architectural choice, and confirming the need for data time-series integrity metrics in subsequent evaluation.

The contribution of this study is a replicable architecture for small-scale hydroponic nutrient supply automation with concentration-threshold dosing, RTC-backed local scheduling, IoT-based remote visibility, and PV-based energy autonomy with LiFePO4 storage. The system suits educational and household baselines because it demonstrates embedded control, local timekeeping, pump actuation, smartphone monitoring, and photovoltaic supply design with readily available components while providing power capacity reserve for expansion. The key energy finding is that inverter operating strategy and battery chemistry selection, not solar module capacity, are the most decisive factors for system efficiency and autonomy. The results must not be interpreted as evidence of nutrient dosing accuracy, measured PV performance, or improved plant growth. Stronger contributions require calibrated sensing, pH/EC or TDS monitoring, flow rate and nutrient volume validation, communication performance measurement, irradiance and inverter standby logging, BMS-reported state of charge, power and cost analysis, and controlled plant growth trials, together with scalability testing across multiple hydroponic units and more capable controllers.

V. ACKNOWLEDGEMENTS

The authors thank the Ministry of

10.21070/jeeeu.v10i2.1758

Higher Education, Science, and Technology of the Republic of Indonesia for funding this research, and the Rector and the Institute for Research and Community Service (LPPM) of Universitas Darul Ulum, Jombang, for technical support during the preparation of this manuscript.

VI. REFERENCES

[1] C. Maraveas, D. Piromalis, K. G. Arvanitis, T. Bartzanas, and D. Loukatos, "Applications of IoT for optimized greenhouse environment and resources management," Comput. Electron. Agric., vol. 198, art. no. 106993, 2022, doi: 10.1016/j.compag.2022.106993.

[2] A. A. Abdelmoneim, H. N. Kimaita, C. M. Al Kalaany, B. Derardja, G. Dragonetti, and R. Khadra, "IoT sensing for advanced irrigation management: A systematic review of trends, challenges, and future prospects," Sensors, vol. 25, no. 7, art. no. 2291, 2025, doi: 10.3390/s25072291.

[3] M. A. Rahman, N. R. Chakraborty, A. Sufiun, S. K. Banshal, and F. R. Tajnin, "An AIoT-based hydroponic system for crop recommendation and nutrient parameter monitorization," Smart Agric. Technol., vol. 8, art. no. 100472, 2024, doi: 10.1016/j.atech.2024.100472.

[4] K. Duangpakdee, G. Thananta, and S. Sukpancharoen, "IoT enhanced deep water culture hydroponic system for optimizing Chinese celery yield and economic evaluation," Smart Agric. Technol., vol. 9, art. no. 100545, 2024, doi: 10.1016/j.atech.2024.100545.

[5] T. Demir and I. Cicek, "A low-cost and reliable IoT-based NFT hydroponics system using ESP32 and MING stack," Eng. Proc., vol. 122, no. 1, art. no. 3, 2026.

[6] S. Harishankar, R. S. Kumar, K. P. Sudharsan, U. Vignesh, and T. Viveknath, "Solar powered smart irrigation system," Adv. Electron. Electr. Eng., vol. 4, no. 4, pp. 341–346, 2014.

[7] T. Khatib, A. Mohamed, and K. Sopian, "A review of photovoltaic systems size optimization techniques," Renew. Sustain. Energy Rev., vol. 22, pp. 454–465, 2013, doi: 10.1016/j.rser.2013.02.023.

[8] M. F. Aranda Barrera and H. Ponce, "Modular IoT hydroponics system," Horticulturae, vol. 11, no. 11, art. no. 1306, 2025, doi: 10.3390/horticulturae11111306.

[9] A. Abu Sneineh and A. A. A. Shabaneh, "Design of a smart hydroponics monitoring system using an ESP32 microcontroller and the Internet of Things," MethodsX, vol. 11, art. no. 102401, 2023, doi: 10.1016/j.mex.2023.102401.

[10] H. Sulaiman, A. A. Yusof, and M. K. Mohamed Nor, "Automated hydroponic nutrient dosing system: A scoping review of pH and electrical conductivity dosing frameworks," AgriEngineering, vol. 7, no. 2, art. no. 43, 2025, doi: 10.3390/agriengineering7020043.

[11] K. K. Y. Shin, T. P. Ping, M. G. B. Ling, C. Chee Jiun, and N. A. B. Bolhassan, "SMART GROW – Low-cost automated hydroponic system for urban farming," HardwareX, vol. 17, art. no. e00498, 2024, doi: 10.1016/j.ohx.2023.e00498.

[12] P. Megantoro, R. P. Prastio, H. F. A. Kusuma, A. Abror, P. Vigneshwaran, D. F. Priambodo, and D. S. Alif, "Instrumentation system for data acquisition and monitoring of hydroponic farming using ESP32 via Google Firebase," Indones. J. Electr. Eng. Comput. Sci., vol. 27, no. 1, pp. 52–61, 2022, doi: 10.11591/ijeecs.v27.i1.pp52-61.

[13] M. Sportelli, D. La Rosa, A. Crivello, D. Pineda-Medina, M. Bacco, and P. Barsocchi, "Beyond prototypes: What is missing to fill the gaps in IoT-enabled hydroponics platforms," Horticulturae, vol. 11, no. 11, art. no. 1322, 2025, doi: 10.3390/horticulturae11111322.

[14] Aosong Electronics Co., Ltd., "DHT11 humidity and temperature sensor," datasheet, Mouser Electronics, Guangzhou, China, n.d.

[15] Analog Devices, "DS3231 extremely accurate I2C-integrated RTC/TCXO/crystal," datasheet, Rev. 10, Analog Devices, Wilmington, MA, USA, 2015.

[16] H. J. El-Khozondar, S. Y. Mtair, K. O. Qoffa, O. I. Qasem, A. H. Munyarawi, Y. F. Nassar, E. H. E. Bayoumi, and A. A. E. B. A. El Halim, "A smart energy monitoring system using ESP32 microcontroller," e-Prime – Adv. Electr. Eng. Electron. Energy, vol. 9, 2024.

[17] A. A. Firdaus, F. C. S. Arisgraha, I. Oktamaulana, T. T. Subekti, D. O. Anggriawan, M. Ali, and D. F. U. Putra, "Design of greenhouse monitoring for hydroponic based on microcontroller and android system," in AIP Conf. Proc., vol. 2484, 2023, art. no. 040008.

[18] S. S. Shanto, M. Rahman, J. M. Oasik, and H. Hossain, "Smart greenhouse monitoring system using Blynk IoT app," J. Eng. Res. Rep., vol. 25, no. 2, pp. 94–107, 2023.

[19] J. G. Bea and C. A. D. Bea, "Interfacing Blynk IoT platform for monitoring temperature and humidity in poultry farm," Int. J. Innov. Sci. Res. Technol., vol. 8, no. 6, pp. 3240–3242, 2023.

[20] R. Zaghlool Mahmood, "High accurate automatic school bell controller based on ESP-32 Wi-Fi," Technium Rom. J. Appl. Sci. Technol., vol. 4, no. 10, pp. 126–144, 2022.

[21] M. R. Gundavarapu, V. Swapna, E. S. Reddy, P. P. Kumar, A. Prathapani, and K. Shivaji, "IoT-enhanced smart bulletin board: A multi-

functional connectivity hub," in Proc. 2nd Int. Conf. Intell. Data Commun. Technol. Internet Things (IDCIoT), 2024, pp. 1700–1704.

[22] D. Linden and T. B. Reddy, Handbook of Batteries, 3rd ed. New York, NY, USA: McGraw-Hill, 2002.

[23] G. Yascaribay, M. Huerta, M. Silva, and R. Clotet, "Performance evaluation of communication systems used for Internet of Things in agriculture," Agriculture, vol. 12, no. 6, art. no. 786, 2022, doi: 10.3390/agriculture12060786.

*Corespondent e-mail addres liaundarjombang@gmail.com

Received:2025-09-23
Accepted:2026-04-28
Published:2026-07-02

JEEE-U Journal of Electrical and Electronic Engineering-UMSIDA
ISSN 2460-9250 (print), ISSN 2540-8658 (online)
Vol. 10, No. 2, October 2026
10.21070/jeeeu.v10i2.1758

LIST OF FIGURE

Journal of Electrical and Electronic Engineering-UMSIDA
ISSN 2460-9250 (print), ISSN 2540-8658 (online)
Vol. 10, No. 2, October 2026
10.21070/jeeeu.v10i2.1758

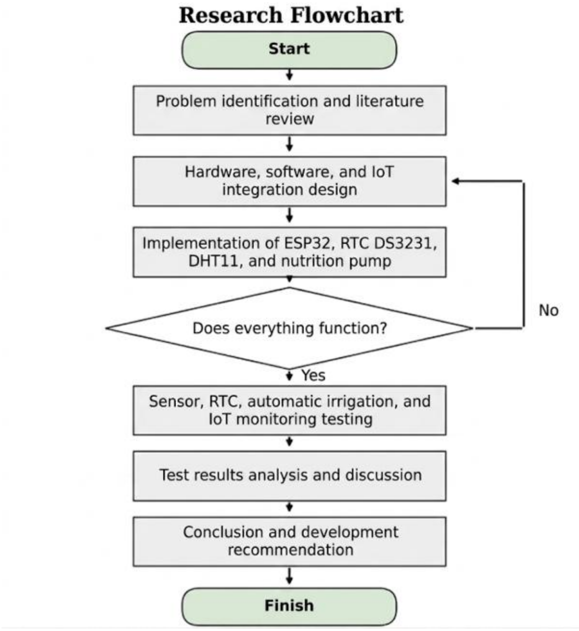

Figure 1. Research flow for design

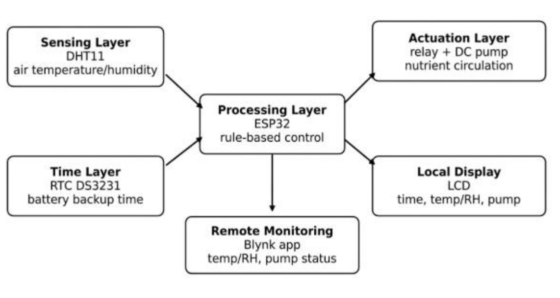

Figure 2. Local-first, solar-powered IoT architecture with RTC-based scheduling

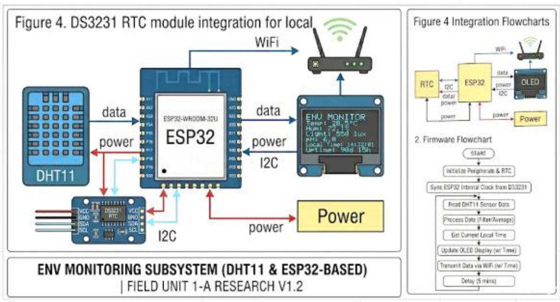

Figure 3. DHT11- and ESP32-based environmental monitoring subsystem, and DS3231 RTC integration for local timekeeping

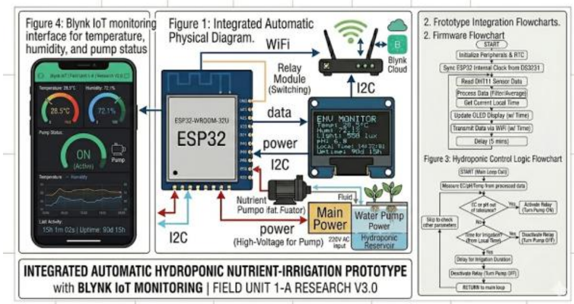

Figure 4. Integrated hydroponic nutrient supply automation prototype with relays, pumps, solar power supply, and the Blynk IoT monitoring interface

JEEE-U Journal of Electrical and Electronic Engineering-UMSIDA
ISSN 2460-9250 (print), ISSN 2540-8658 (online)
Vol. 10, No. 2, October 2026
10.21070/jeeeu.v10i2.1758

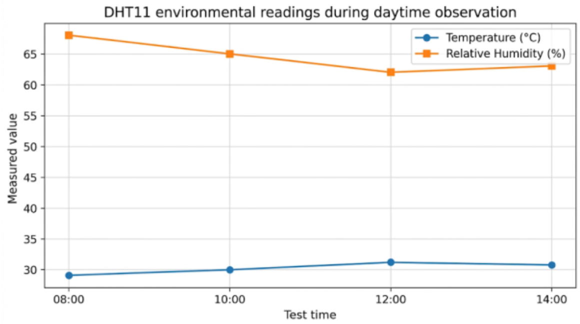

Figure 5. DHT11 temperature and humidity trend during the daytime observation window

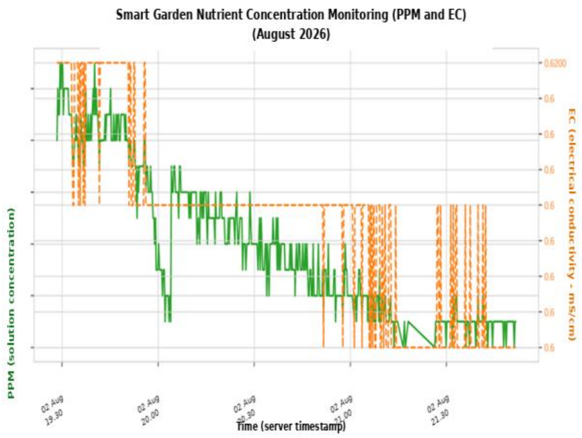

Figure 6. Smart Garden monitoring of (a) temperature and humidity and (b) nutrient concentration (PPM and EC)

JEEE-U Journal of Electrical and Electronic Engineering-UMSIDA
ISSN 2460-9250 (print), ISSN 2540-8658 (online)
Vol. 10, No. 2, October 2026
10.21070/jeeeu.v10i2.1758

LIST OF TABLE

JEEE-U Journal of Electrical and Electronic Engineering-UMSIDA
ISSN 2460-9250 (print), ISSN 2540-8658 (online)
Vol. 10, No. 2, October 2026
10.21070/jeeeu.v10i2.1758

Component	Function in the prototype	Rationale
ESP32 development board	Main controller; reads sensors, processes RTC time, drives relays, sends data to Blynk	Integrated Wi-Fi and programmable GPIO resources for IoT prototyping
DS3231 RTC module	Battery-backed local timekeeping for irrigation scheduling	Preserves schedule execution without full reliance on cloud or network time
DHT11 sensor	Air temperature and relative humidity monitoring	Low-cost contextual monitoring; not used for dosing control
TDS sensor	Measures nutrient concentration in ppm	Makes concentration a control variable, not merely a monitored variable
Relay module	Switches pumps according to ESP32 output	Electrically isolates control signals from pump switching
40 W submersible pump and nutrient dosing pumps	Circulate water and deliver concentrates A and B	Realise nutrient supply with very small daily energy consumption
LCD module	Local display of time, temperature, humidity, and pump status	Allows direct inspection near the prototype
Blynk IoT dashboard	Remote display of temperature, humidity, and pump status	Smartphone-based supervision during testing
450 Wp solar module	Primary energy generator of the automation system	Adequate for daily load and provides reserve for expansion
MPPT SCC 20-30 A, 24 V bus	Regulates LiFePO4 charging; overcharge and over-discharge protection	MPPT with LiFePO4 profile (absorption about 28.8 V) suits the 450 Wp module voltage
LiFePO4 8S 25.6 V 100 Ah (2,560 Wh)	Stores energy for night and cloudy-day operation	80% DoD and high cycle life give 2,048 Wh usable energy and longer autonomy than lead-acid
Taffware 3,000 W inverter (15 W standby)	Provides 220 V AC for the submersible pump and other AC loads	Accommodates pump starting surge and provides expansion headroom
DC-DC converter 24 V to 5 V	Powers ESP32, sensors, and LCD from the	Keeps the control layer alive even when the inverter

10.21070/jeeeu.v10i2.1758

	DC bus	is off

Table 1. Prototype components, including the solar power subsystem, and their functional roles

Step	Operation	Expected output
1	Initialise ESP32, LCD, DHT11, DS3231, relay pins, Wi-Fi, and Blynk connection	Device ready for monitoring and control
2	Read current date and time from DS3231	Local time reference available
3	Read DHT11 temperature and humidity; read TDS concentration	Contextual and control data available
4	Compare time with the 07:00 and 16:00 schedule; compare TDS with the 400 ppm threshold	Event condition TRUE or FALSE
5	If TRUE, energise relay and pump for the programmed duration	Nutrient or water pump runs as programmed
6	De-energise relay and pump after the programmed duration	Pump returns to the off state
7	Update LCD and send variables to Blynk, Telegram, and the spreadsheet log when Wi-Fi is available	Local and remote monitoring information updated
8	Repeat the program loop	Scheduled operation continues indefinitely

Table 2. Rule-based control sequence implemented on the prototype

Validation dimension	Test procedure	Metric	Interpretation
DHT11 display consistency	Record temperature and humidity at 08:00, 10:00, 12:00, and 14:00; compare LCD, Serial Monitor, and Blynk	Mean, range, sample standard deviation, coefficient of variation, display agreement	Whether the monitoring subsystem gives stable readings and consistent displays
RTC timekeeping consistency	Compare DS3231 time with the intended reference over five observation days	Time error = absolute difference between RTC time and reference time; mean absolute time error	Whether the local RTC maintains the programmed irrigation schedule in the short term
Pump actuation	Observe relay and pump state at scheduled ON events and the subsequent	Schedule execution success and actuation reliability	Whether the ESP32-relay-pump chain follows the programmed logic

JEEE-U Journal of Electrical and Electronic Engineering-UMSIDA
ISSN 2460-9250 (print), ISSN 2540-8658 (online)
Vol. 10, No. 2, October 2026
10.21070/jeeeu.v10i2.1758

	OFF state		
IoT monitoring	Observe Wi-Fi connection and Blynk display of temperature, humidity, and pump status	Monitoring availability and transmission status, qualitatively	Whether remote supervision is available during prototype testing
Solar power adequacy	Compute daily energy balance from component specifications and nominal load profile	Daily energy demand (Wh/day), PV production potential (Wh/day), energy adequacy ratio, battery autonomy (days)	Whether module and battery capacity can sustain nutrient supply without the grid

Table 3. Prototype evaluation dimensions and metrics

No.	**Test time**	**Temperature (degrees Celsius)**	**Humidity (%)**
1	08:00	29.1	68
2	10:00	30.0	65
3	12:00	31.2	62
4	14:00	30.8	63
Parameter	Mean	Min - Max (range)	SD / CV
Temperature	30.28 degrees Celsius	29.1 - 31.2 (2.1 degrees Celsius)	0.93 / 3.08%
Relative humidity	64.50%	62 - 68% (6%)	2.65% / 4.11%

Table 4. DHT11 test results and descriptive statistics

No.	**Observation time**	**Expected state**	**Observed state**	**Duration**	**Remark**
1	07:00:00	ON	ON	10 s	Operating
2	07:00:10	OFF	OFF	-	Normal
3	16:00:00	ON	ON	10 s	Operating
4	16:00:10	OFF	OFF	-	Normal

Table 5. Automatic nutrient supply test results

Device	**Category**	**Main function**	**Role in control logic**
TDS meter	Sensing	Measures nutrient concentration in ppm	Primary control variable; triggers dosing below 400 ppm
DHT11	Sensing	Measures air temperature	Monitoring only; contextual interpretation

JEEE-U Journal of Electrical and Electronic Engineering-UMSIDA
ISSN 2460-9250 (print), ISSN 2540-8658 (online)
Vol. 10, No. 2, October 2026
10.21070/jeeeu.v10i2.1758

		and humidity	
DS3231 RTC and NTP on ESP32	Time reference	Local timekeeping and online time synchronisation	Dual reference; RTC preserves schedule offline, NTP corrects drift online
Nutrient pump A / pump B	Actuation	Deliver concentrates A and B	Run alternately in the automatic dosing cycle
40 W submersible pump	Actuation	Irrigates or circulates the nutrient solution	Runs on schedule at 07:00 and 16:00 for 1 min; about 1.3 Wh/day
450 Wp module and 24 V MPPT SCC	Power supply	Generates and regulates system energy	Supplies control and actuation chains without the grid
LiFePO4 8S 25.6 V 100 Ah	Power supply	Stores energy for night and cloudy days	Sustains scheduling and dosing without insolation; BMS protects cells
Taffware 3,000 W inverter	Power conversion	Converts battery DC to 220 V AC	Relay-switchable so the 15 W standby loss does not burden the energy balance

Table 6. Smart Garden sensor and actuator configuration and control roles

Parameter	**Observed range**	**Main logging window**	**Interpretation**
Air temperature	28.6-30.0 degrees Celsius	2 August (intensive), continuing to 6 August	Reasonable daily fluctuation; peak at 30.0 degrees Celsius
Relative humidity	About 60-71%	2 August (intensive), continuing to 6 August	Tends to correlate negatively with temperature
Nutrient concentration (PPM)	About 397 down to 386	2 August, 19:28-21:51	Gradual decline of about 11 ppm (about 2.8%)
Electrical conductivity (EC)	0.6000-0.6200 mS/cm	2 August, 19:28-21:51	Moves identically with PPM per the conversion factor
Server data integrity	Gap between 2 and 6 August	Whole period	Logging gap in the data transmission chain

Table 7. Summary of Smart Garden field monitoring parameters

JEEE-U Journal of Electrical and Electronic Engineering-UMSIDA
ISSN 2460-9250 (print), ISSN 2540-8658 (online)
Vol. 10, No. 2, October 2026
10.21070/jeeeu.v10i2.1758

Aspect	Prototype testing	Field monitoring	Synchronisation conclusion
Air temperature	29.1-31.2 degrees Celsius; mean 30.28 (4 observations)	28.6-30.0 degrees Celsius (high-density time series)	Overlapping and consistent; field monitoring widens temporal coverage
Relative humidity	62-68%; mean 64.50%	About 60-71%	Consistent; wider field range due to longer observation period
Nutrient solution quality	Not measured (stated limitation)	PPM about 397 to 386; EC 0.6000-0.6200 mS/cm	Partly closes the pH/EC/TDS sensing limitation
Local time reference	RTC error 0 s over 5 days	Server timestamps remain ordered in each logging session	Local timekeeping confirmed reliable in the short term
Data delivery reliability	Qualitative: Blynk available during testing	Logging gap 2-6 August	Limitation lies in the network/server layer, not local scheduling
Pump actuation	100% schedule execution and actuation reliability	Recorded nutrient concentration decline	Actuation demonstrably affects the solution; dose quantification still needs a flow sensor
Solar power supply	Designed and computed via energy balance (about 1,350 Wh/day production; 42-398 Wh/day load)	System operated throughout logging with no recorded power interruption	Energy adequacy indicated but quantitative verification needs irradiance, charging current, inverter standby, and BMS state-of-charge logging

Table 8. Synchronisation of prototype testing (Subsections 3.2-3.6) and field monitoring (Subsection 3.7)